Effect of Curvature of Coating Die Edges on the Pinning of Contact Line

Oldrich Joel Romero
Dept. of Mechanical Engineering, Pontificia Universidade Catolica do Rio de Janeiro, Rua Marques de Sao Vicente 225, Gavea, Rio de Janeiro, RJ, 22453–900, Brazil

L. E. Scriven
Dept. of Chemical Engineering and Materials Science, University of Minnesota, MN 55455

Márcio da Silveira Carvalho
Dept. of Mechanical Engineering, Pontificia Universidade Catolica do Rio de Janeiro, Rua Marques de Sao Vicente 225, Gavea, Rio de Janeiro, RJ, 22453–900, Brazil

DOI 10.1002/aic.10672
Published online September 19, 2005 in Wiley InterScience (www.interscience.wiley.com).

Coating die edges are not mathematical corners, they are rounded. Contact lines do not actually pin. The effects of the radius of curvature of the downstream edge of slot dies on contact line location, effective contact angle, and low-flow limit—air-fingers penetrating from downstream and breaking apart the coating-bead—are examined by solving the Navier-Stokes system for Newtonian flow. The geometry of the die surface is represented by two straight lines and an arc of circle connecting them. The local contact angle is treated as a specified equilibrium value. The system of equations is solved by Galerkin's method and finite element basis functions. The results show how the edge rounding affects the contact line position and stability of the flow, and indicate the minimum radius of curvature necessary to apparently pin the contact line. © 2005 American Institute of Chemical Engineers *AIChE J,* 52: 447–455, 2006
Keywords: slot coating, contact line, low-flow limit, die edges

Introduction

Slot coating is commonly used in the manufacturing of adhesive and magnetic tapes, specialty papers, imaging films, and many other products. In this process, the coating liquid is pumped to a coating die in which an elongated chamber distributes it across the width of a narrow slot through which the flow rate per unit width at the slot exit is made uniform. Exiting the slot, the liquid fills (wholly or partially) the gap between the adjacent die lips and the substrate translating rapidly past them. The liquid in the gap, bounded upstream and downstream by gas-liquid interfaces, or menisci, forms the coating bead, as shown in Figure 1. In order to sustain the coating bead at higher substrate speeds, the gas pressure upstream of the upstream meniscus is made lower than ambient, i.e., a slight vacuum is applied to the upstream meniscus (Beguin[1]). Slot coating belongs to a class of coating methods known as "pre-metered coating": the thickness of the coated liquid layer is set by the flow rate fed to the coating die and the speed of the moving substrate, and is independent of other process variables. Thus, pre-metered methods are ideal for high precision coating. However, the nature of the flow in the coating bead and the uniformity of the liquid layer it delivers can be affected by the substrate speed, liquid properties, configuration of the die lips, and cross-web uniformity of the contact lines position.

The region in the space of operating parameters of a coating

Correspondence concerning this article should be addressed to M.S. Carvalho at msc@mec.puc-rio.br.

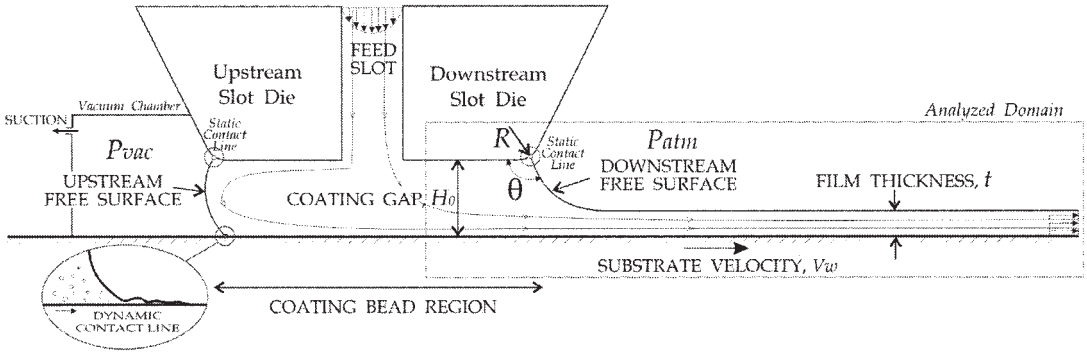

Figure 1. Slot coating process.

process where the delivered liquid layer is adequately uniform is usually referred to as a "coating window." Knowledge of coating windows of different coating methods is needed in order to predict whether a particular method can be used to coat a given substrate at a prescribed production rate. Coating windows can be constructed either by extensive and expensive experimentation or from theoretical modeling of the coating flow at relatively low cost.

Romero et al.[2] reviews the different analysis of slot coating flows and predictions of the coating window of the process for both Newtonian and non-Newtonian liquids. The main contributions for Newtonian flows are by Ruschak,[3] Silliman,[4] Higgins and Scriven,[5] Sartor,[6] Gates,[7] and Carvalho and Kheshgi.[8] They show that for low viscosity liquids, the most important limit in the slot coating process occurs when, at a given substrate speed, too low flow rate per unit width from the slot causes the downstream meniscus to curve so much that it cannot bridge the gap's clearance H_0. Consequently, the meniscus becomes progressively more three-dimensional, alternate parts of it invading the gap until the bead takes a form that delivers separate rivulets or chains of droplets to the substrate moving past, as illustrated in Figure 2. This transition from a continuous coated liquid layer is what is called here the "low-flow limit": the minimum thickness of liquid that can be deposited from a gap of specified clearance at a given substrate speed. It is independent of the vacuum applied, given that the vacuum is great enough to draw the upstream meniscus away from the feed slot. The coating window of the process when the low-flow limit is the principal mechanism of failure is sketched in Figure 3.

The theoretically determined low-flow limit is defined by Carvalho and Kheshgi,[8] Romero et al.,[2] and Romero et al.[9] as the flow rate at which the static contact angle θ between the downstream free surface and the downstream die lip becomes less than 10°. Their analyses assume that the downstream free surface is pinned at the corner between the downstream die lip and shoulder. This is a simplified view of the problem, because corners are not mathematical and contact lines do not actually pin.

In practice, it is important that the location of the contact line is uniform in the transverse direction to guarantee a two-dimensional flow. Oliver et al.[10] have shown that if a solid wall has an edge, or any other type of non-uniformity, the contact angle hysteresis is enhanced, reducing the wetting line mobility. Therefore, if the coating die surface has an edge, the contact line may preferentially locate along it: It is common practice in the coating industry to use edges on the coating applicators to "pin" a wetting line, as described by Maier and Brown[11] and Fahrni and Zimmermann.[12]

In principle, the contact line remains on the edge for a range of contact angles θ given by the Gibbs inequality condition[13]:

$$\theta_R < \theta < \theta_A + 180^\circ - \gamma \qquad (1)$$

where θ, the contact angle, is measured through the liquid phase. The receding contact angle θ_R is the smallest angle

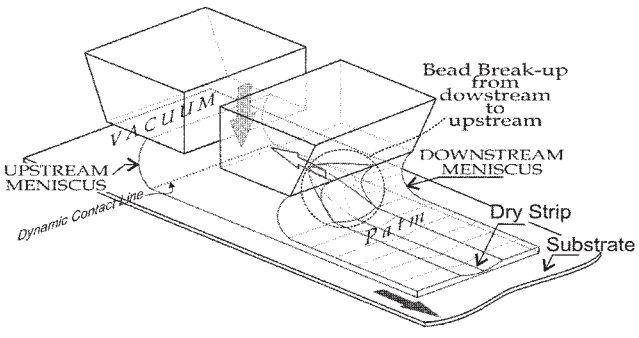

Figure 2. Three-Dimensional sketch of the bead break-up from the upstream meniscus, which marks the onset of the low-flow limit in the slot coating process.

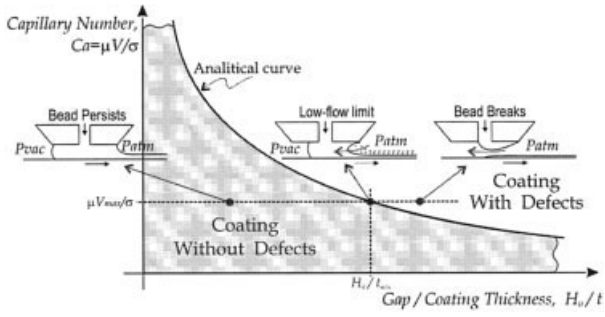

Figure 3. Coating window of the slot coating process in the plane capillary number *Ca* vs. gap-to-thickness ratio H_o/t.

The solid line represents the minimum film thickness t_{min} that can be deposited without defects onto the substrate in movement at a given capillary number.

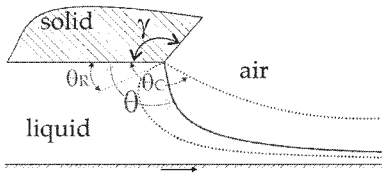

Figure 4. Geometrical representation of the Gibbs' condition $\theta_R < \theta < \theta_C$, where $\theta_C = \theta_A + 180^o - \gamma$.

achievable before the wetting line begins to move in the direction of the liquid phase. The advancing contact angle θ_A is the largest angle before the wetting line begins to move in the direction of the air phase. γ is the solid edge angle, as shown in Figure 4. The sharper this angle, the greater the hysteresis and the smaller is the wetting-line mobility. This is also a simplified view of the problem, because coating die edges are not mathematical corners and contact lines do not actually pin. As stated by Oliver et al.,[10] ". . . it is probably more realistic to consider an edge as a continuous surface without singularities; i.e., it is rounded with a radius of curvature $R \neq 0$, so that the contact angle measured to the tangent of the surface (at the submicroscopic level) presumably could remain constant, provided of course that the solid surface is isotropic and energetically homogeneous. . . " A schematic representation of this concept is shown in Figure 5.

Edges in coating dies have a specified radius of curvature. The lower limit of its value is set by limitations on the machining process. Special procedures are used to reduce the radius of curvature of coating applicators, as described by Yapel et al.[14] In this work, the effect of the radius of curvature of the edge between the downstream die lip and die shoulder on the position of the contact line and on the critical conditions at the onset of the low-flow limit is examined by solving the Newtonian flow in the downstream part of the coating bead, as shown in Figure 1. The contact angle is treated as a specified equilibrium value and the static contact line position is free to move along the surface of the die lip, die edge, and die shoulder. The system of differential equations and boundary conditions is solved by the Galerkin/Finite Element Method. At each operating condition (liquid properties as well as coating gap and web speed), a sequence of states is found by Newton's iterations initialized by first-order, pseudo-arc-length continuation, i.e., a solution path in the parameter space is constructed as the flow rate to the die falls.

Mathematical Formulation

The flow in the coating bead is described by the two-dimensional, steady state mass and momentum conservation equations for Newtonian liquid.

Carvalho and Kheshgi,[8] Romero et al.,[2] and Romero et al.[9] have shown that at low capillary and Reynolds numbers, the flow upstream of the feed slot does not affect the critical operating conditions at the onset of the low-flow limit. Because the analysis presented here focuses on the effect of the radius of curvature of the edge of the downstream slot die at low capillary number and vanishing Reynolds number, the flow domain in which the governing equations are solved is truncated to the region adjacent to the downstream free surface.

The geometry of the die surface consists of two straight lines, which represent the die lip and the die shoulder surfaces, connected by an arc of circle, as sketched in Figure 6. Three different radii of curvature of the die edge are analyzed: $R = 200\ \mu$m; $R = 100\ \mu$m, and $R = 50\ \mu$m. The inclination of the die shoulder with respect to the web is fixed at $\alpha_S = 45^o$. Three different angles between the die lip and the substrate are examined, that is, $\alpha_L = -2.86°$; $\alpha_L = +2.86$ and $\alpha_L = 0^o$, which correspond to a convergent, divergent, and parallel flow channel under the die lip. In all the die configurations, H_0 is the distance of the die lip to the moving web at the intersection of the straight line that represents the die lip with the arc of circle that represents the rounded edge, as indicated in Figure 6. The obligatory synthetic inflow boundary is a plane placed at $10H_0$ upstream of the point where the two straight lines that represent the die lip and shoulder meet. The similarly obligatory outflow plane is placed $15H_0$ downstream of that same point. Tests confirmed that shifting these planes further upstream and downstream has negligible effect on the results. The ratio of the downstream die lip length (L) to the coating gap in some industrial applications is in the same order of magnitude as the one used here, i.e., $L/H_0 \approx 10$.

The velocity $\mathbf{v}$ and pressure p fields of 2D Stokes flow are governed by the continuity and Stokes equations for incompressible Newtonian liquid:

$$\nabla \cdot \mathbf{v} = 0, \quad -\nabla p + \mu \nabla^2 \mathbf{v} = \mathbf{0}, \tag{2}$$

where μ is the liquid viscosity.

The boundaries of the flow domain are labeled in Figure 7, and the correspondent boundary conditions are:

(1) *Inflow*: Fully developed parallel rectilinear flow,

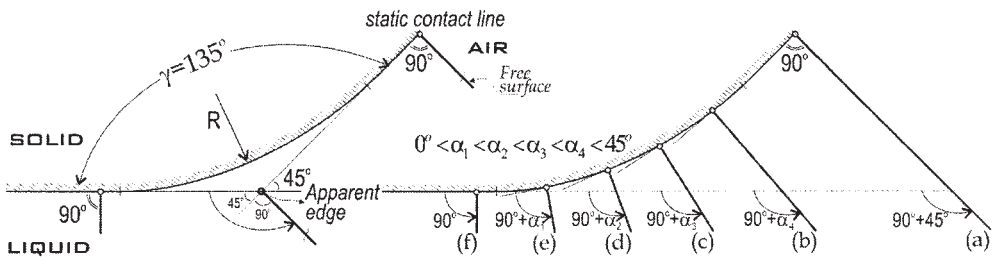

Figure 5. Schematic representation of the static contact line sliding along the rounded edge, adapted from Oliver et al.[10] The free surface is represented as a straight line corresponding at the conditions (a), (b). . . (f) of Figure 12. Capillary number is kept constant at $Ca = 0.17$.

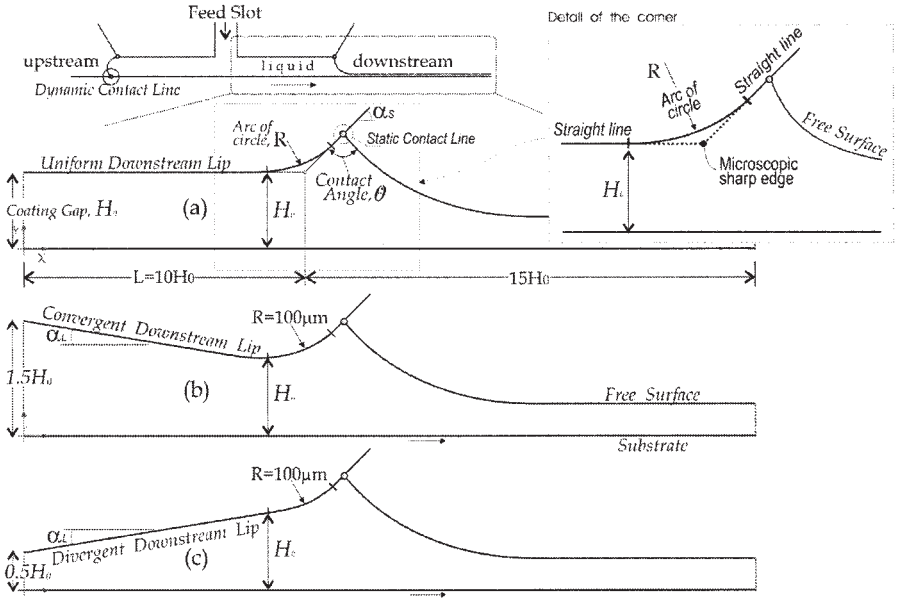

Figure 6. Detail of the downstream slot die showing the three gap configurations used in this work.

(a) Uniform ($\alpha_L = 0^o$), (b) convergent ($\alpha_L = +2.86^o$), and (c) divergent ($\alpha_L = -2.86^o$). A zoom close to the rounder edge is also shown in the top right corner of the figure.

Couette-Poiseuille velocity profile.

$$u = \frac{6V_w t}{H_0}\left[\left(-1+\frac{1}{2}\frac{H_0}{t}\right)\left(\frac{y}{H_0}\right)^2 + \left(-1+\frac{2}{3}\frac{H_0}{t}\right)\left(\frac{y}{H_0}\right)+\frac{1}{6}\frac{H_0}{t}\right], \quad v = 0. \tag{3}$$

V_w is the substrate velocity, and t is the coating thickness; both are input parameters.

(2) *Moving substrate*: No-slip, no-penetration.

$$u = V_w, \quad v = 0. \tag{4}$$

(3) *Outflow*: Fully developed flow.

$$\mathbf{n}\cdot\nabla\mathbf{v} = 0, \tag{5}$$

$\mathbf{n}\cdot\nabla$ is the directional derivative parallel to the substrate.

(4) *Free surface*: Force balance and kinematic condition.

$$\mathbf{n}_{fs}\cdot\mathbf{T} = \sigma\frac{d\mathbf{t}_{fs}}{ds} - \mathbf{n}_{fs}p_{amb}, \tag{6}$$

$$\mathbf{n}\cdot\mathbf{v} = 0, \tag{7}$$

$\mathbf{t}_{fs}$ and $\mathbf{n}_{fs}$ are the local unit tangent and unit normal to the free surface, s is the arc-length coordinate along the interface, $\mathbf{T}$ is the liquid stress tensor for Newtonian liquid, σ is the liquid surface tension, and p_{amb} is the ambient pressure.

(5) *Static contact line*: The contact line is free to move with a prescribed contact angle.

$$\mathbf{n}_w\cdot\mathbf{n}_{fs} = \cos(\theta), \tag{8}$$

θ is the angle between the free surface unit normal vector $\mathbf{n}_{fs}$ and the die surface unit normal vector $\mathbf{n}_w$. Two values of the contact angle are considered: $\theta = 90^o$ and $\theta = 45^o$.

(6) *Die land*: No-slip, no-penetration.

$$\mathbf{v} = 0. \tag{9}$$

The important dimensionless parameters are:

- Capillary number *Ca*:

$$Ca \equiv \frac{\mu V_w}{\sigma}, \tag{10}$$

which measures the ratio of viscous to capillary forces.

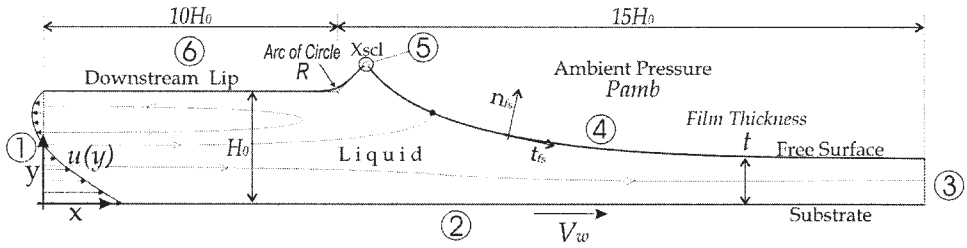

Figure 7. Sketch of the flow domain with the boundary conditions.

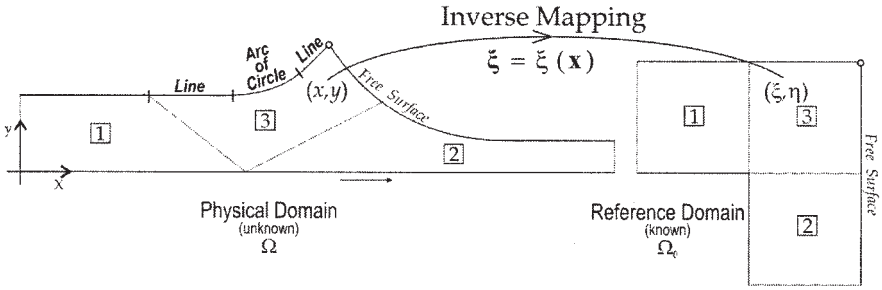

Figure 8. Mapping from the physical to the reference domain.

- Gap-to-Thickness ratio h:

$$h \equiv \frac{H_0}{t}. \tag{11}$$

Solution Method

Because of the free surface, the flow domain is unknown a priori. Capillary forces are comparable to viscous forces in coating flows; fully coupled solution methods—the position of the interface and the flow solution are computed simultaneously—are superior to the fixed-point iterative method, where the domain shape and the flow are computed alternatively. Fully coupled methods rely on mapping the unknown physical domain Ω into a known reference domain Ω_0 by means of a bijective transformation $\mathbf{x} = \mathbf{x}(\boldsymbol{\xi})$, where $\mathbf{x}$ and $\boldsymbol{\xi}$ denote position in the physical and reference domain, respectively. The mapping used here is the one described by de Santos[15] and represented in Figure 8. The inverse of the mapping $-\boldsymbol{\xi} = \boldsymbol{\xi}(\mathbf{x})-$ is governed by a pair of elliptic differential equations identical to those encountered in diffusional transport with variable diffusion coefficients. The coordinate potentials ξ and η of the reference domain satisfy:

$$\nabla \cdot (D_\xi \nabla \xi) = 0, \quad \nabla \cdot (D_\eta \nabla \eta) = 0, \tag{12}$$

D_ξ and D_η are diffusion-like coefficients used to control gradients in coordinate potentials, and thereby the spacing between curves of constant ξ on the one hand and of constant η on the other, that make up the sides of the elements that are employed; they are quadrilateral elements. Boundary conditions are needed in order to solve the second-order partial differential equations, Eq. 12. The solid walls and synthetic inlet and outlet planes are described by functions of the coordinates, and along them stretching functions are used to distribute the termini of the coordinate curves selected to serve as element sides. The free boundary (gas-liquid interface) requires imposing the kinematic condition, viz., Eq. 7. The discrete version of the mapping equations is generally referred to as mesh generation equations.

The set of differential equations that describe the conservation of mass and momentum Eq. 2 and define the mapping between the physical and reference domain Eq. 12, together with the appropriate boundary conditions, are all solved on the reference domain Ω_0 by the Galerkin/Finite Element Method. The position and velocity fields are represented as a linear combination of Lagrangian biquadratic basis functions, and the pressure field as a linear combination of linear discontinuous basis functions.

The set of nonlinear algebraic equations that arises from applying the method of weighted residuals and the representation of the variables in terms of basis functions is solved by Newton's method with analytical Jacobian, a first order arc-length continuation (Bolstad and Keller[16]), and a bordering algorithm (Keller[17]). The tolerance of the L_2-norm of the residual vector and the last Newton update for each solution is set to 10^{-6}.

Three different meshes are tested. The coarsest mesh, Mesh 1, has 246 elements and 4,990 degrees of freedom. Mesh 2 has 568 elements and 11,228 degrees of freedom. The finest mesh, Mesh 3, has 960 elements and 18,778 degrees of freedom. Figure 9 shows the tessellation near the free surface for the three meshes. A mesh convergence analysis is also presented; the pressure along the free surface obtained with the three different meshes is compared. The radius of curvature of the die edge is $R = 200$ μm and the imposed contact angle is 90°. The results presented in the next section are computed with Mesh 2, shown in Figure 10.

Results

Theoretical predictions are presented at two different capillary numbers, $Ca = 0.05$ and $Ca = 0.17$. The operating conditions at the low-flow limit are determined theoretically by following a solution path constructed at a fixed capillary number (e.g., fixed substrate velocity, liquid viscosity, and surface tension) by lowering the flow rate, and consequently the thickness of the coated liquid layer. The local contact angle is treated as a specified equilibrium value, and the static contact line position is free to move along the surface of the die.

The flow field as a function of the coated layer thickness is shown in Figure 11 at capillary number $Ca = 0.17$, $\alpha_L = 0°$ (die lip parallel to the substrate), radius of curvature of the die edge $R = 100$ μm, and contact angle $\theta = 90°$. At high flow rates, the static contact line is located on the die shoulder. As the thickness of the deposited liquid falls, the adverse pressure gradient driven flow under the die lip becomes stronger and the static contact line moves towards the die edge. For $H_0/t < 3$, the adverse pressure gradient is not strong enough and there is no recirculation in the flow. As predicted by lubrication approximation, for $H_0/t \geq 3$ a recirculation appears under the die lip. The flow state at $H_0/t = 3.33$ clearly shows the recirculation. As the gap-to-thickness ratio increases even further, the recirculation becomes larger and the meniscus moves toward the inlet plane. At large gap-to-thickness ratio, the sensitivity of

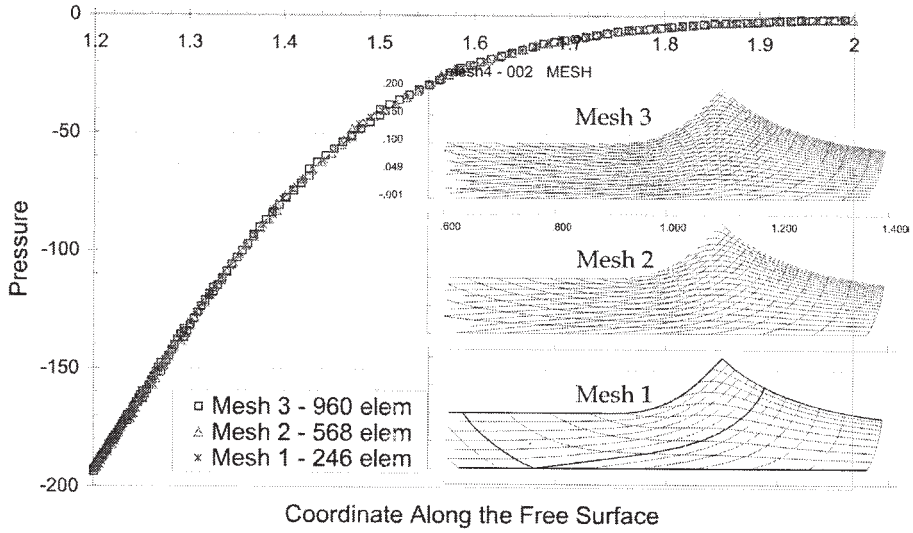

Figure 9. Pressure along the substrate with different meshes in uniform slot coating with radius of the die edge R = 200 μm.

the static contact line position to the film thickness is very strong, as is clear from Figures 11d and e. If the adverse pressure gradient under the die lip is above a critical value, the two-dimensional flow becomes unstable to periodic three-dimensional disturbance, leading to a coating defect known as ribbing. The critical conditions at which this instability appears may be predicted by a linear stability analysis, as the one presented by Gates and Scriven.[7]

The flow states as a function of the coated thickness at R = 200 μm and Ca = 0.17 are shown in Figure 12. The behavior is similar to the one just described; however, the recirculation is at first restricted to a small area adjacent to the free surface.

Figure 13 shows the effect of the contact angle on the flow field at Ca = 0.17 in a parallel coating gap configuration with an edge of curvature of R = 100 μm. At contact angle $\theta = 45^{o}$, the meniscus curvature is more pronounced, leading to a higher pressure jump across the liquid-air interface. As the flow rate increases, the static contact line moves away from the die edge, and the length of the die shoulder that is wet by the liquid rises. In this case there is a large recirculation under the die shoulder. The onset of the recirculation under the die lip is virtually independent of the contact angle and occurs at H_0/t = 3. At the lower contact angle, the recirculation under the die shoulder merges with the one under the die lip, as shown in Figure 13d.

The presence of the recirculation under the die shoulder is a function of the capillary number. Figure 14 shows the flow near the meniscus at $\theta = 90^{o}$, and two capillary numbers, Ca = 0.17 and Ca = 0.05. At low capillary number, the pressure jump across the meniscus is higher, pulling the static contact line downstream. In this case, a recirculation under the die shoulder can be observed. The liquid trapped in the vortex has very high residence time. In industrial applications, solvents may rapidly evaporate, leading to deposition of solids on the coating die, making the static contact line not straight and raising the possibility of nonuniformities in the coated layer. Therefore, recirculations under the die shoulder should be avoided in industrial applications. Experimental evidences of this vortex are presented by Sartor.[6]

Figure 15 shows the contact line position X_{scl} as the flow rate falls, that is, as the gap over film thickness ratio rises, at different die edge radius of curvature R and prescribed contact angles θ. The predictions are obtained at Ca = 0.17 in a parallel flow channel ($\alpha_L = 0^{o}$). The position X_{scl} = 1 corresponds to the sharp edge position, i.e., the corner that is the

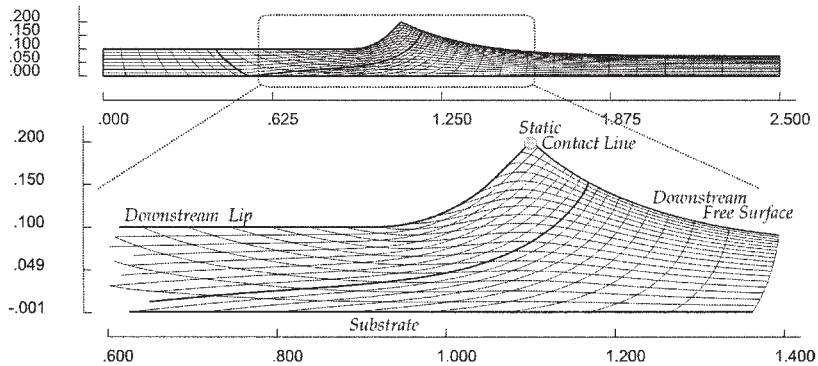

Figure 10. Detail of the mesh used in this work (Mesh 2 with 568 elements) near the free surface for the uniform slot die configuration with R = 200 μm.

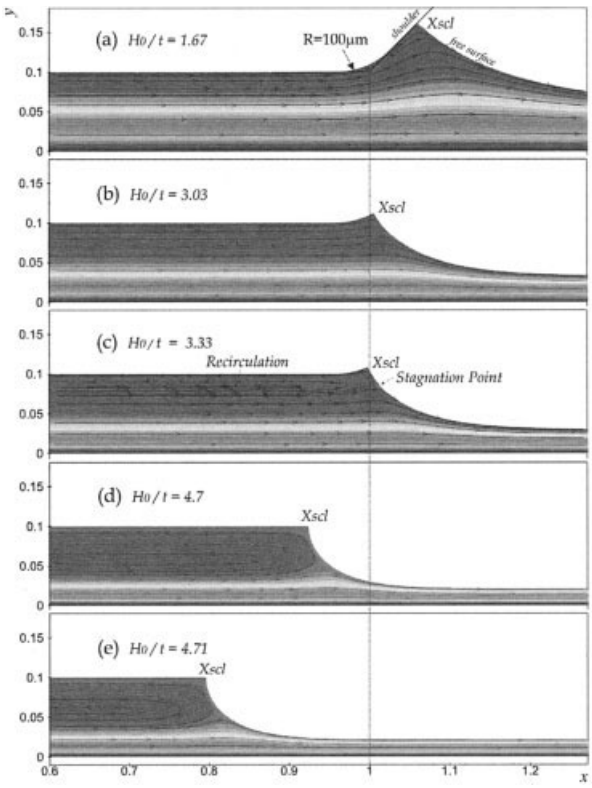

Figure 11. Evolution of the streamlines as the flow rate, that is, film thickness, falls.

Uniform slot coating gap with H_0=100 μm and die edge radius R = 100 μm, prescribed contact angle θ = 90°, and capillary number Ca = 0.17.

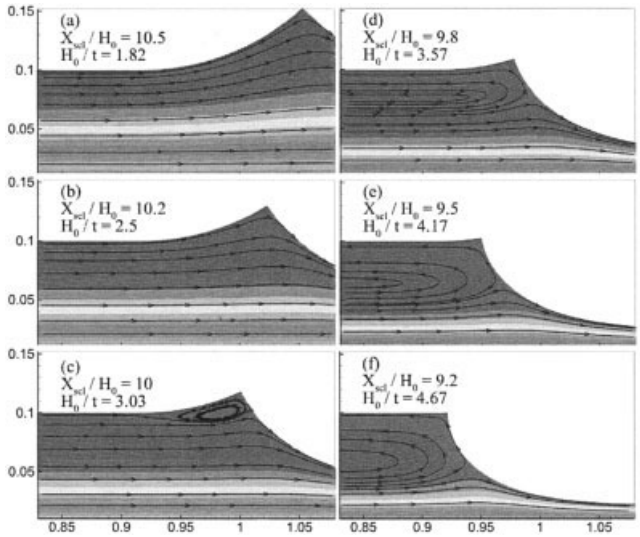

Figure 12. Flow field as a function of flow rate (that is, coating thickness diminishing from (a) to (f)); the detail shows the static contact line X_{scl} sliding along the edge with R = 200 μm in a uniform coating gap with H_0 = 100 μm, static contact angle θ = 90°, and capillary number Ca = 0.17.

intersection of the straight lines that define the die shoulder and die land. When the contact line is taken to be pinned at the corner and the contact angle varies with the flow parameters, as done in the model presented by Carvalho and Kheshgi[8] and Romero et al.[2], θ = 10 is obtained at $H_0/t \approx 7.1$. This is taken to be the critical condition at the onset of the low-flow limit. In the model presented here, the static contact line is free to move along the die surface. At low gap-to-thickness ratio, the contact line is located on the die shoulder ($X_{scl} > 1$). The meniscus moves upstream as the flow rate falls (gap-to-thickness ratio rises), moving from the die shoulder to the rounded edge and then to the die land. The position of the contact line as a function of the coated layer thickness is independent of the radius of curvature of the die edge when it is located over the die shoulder and the die lip. On the other hand, the sensitivity of the contact line position to the flow rate is a strong function of the edge curvature when the contact line is located on the rounded corner. At large radius of curvature, such as, R = 200 μm, there is a large variation of the position X_{scl} as the gap-to-thickness ratio varies from $1.7 \leq H_0/t \leq 4.7$. At the sharper edge, R = 50 μm, the sensitivity of the position of the contact line to the flow rate is weak, indicating an apparent "pinning" effect.

A turning point in the solution path is not found, but a maximum gap-to-thickness ratio of approximately $H_0/t \approx 4.7$ can be asymptotically determined. The radius of curvature of the die edge does not affect this critical value.

The effect of the static contact angle on the low-flow limit (maximum gap-to-thickness ratio) is also presented in Figure 15. A solution path at R = 100 μm and θ = 45° is also shown in the plot. The sensitivity of the contact line position to the flow rate is not strongly affected by the prescribed contact angle, but the contact angle has a strong effect on the onset of the low-flow limit. The critical condition at θ = 45° is $H_0/t \approx$ 6.4.

The flow field as a function of the angle of the die lip with the substrate is shown in Figure 16 at $H_0/t \approx 3.33$. and θ = 90°. At this condition, the contact line is located on the rounded edge. Because $H_0/t > 3$, a recirculation under the die lip is

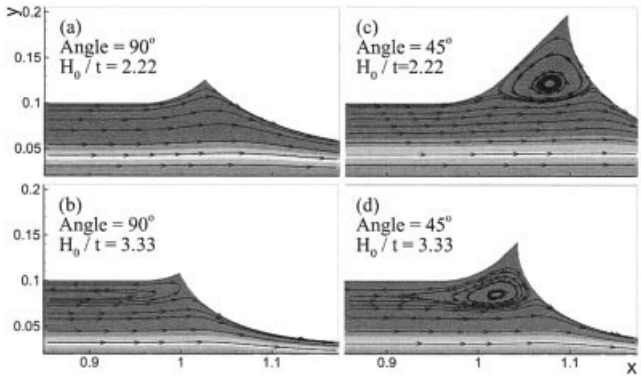

Figure 13. Flow field close to the die with R = 100 μm and α_L = 0°. Recirculations under the die shoulder appear when the static contact angle ("Angle" in the caption) is θ = 45°.

Comparisons are for two different gap-to-thickness ratios, i.e., H_0/t = 2.22 and H_0/t = 3.33, contact angles θ = 90° and θ = 45°, and capillary number Ca = 0.17.

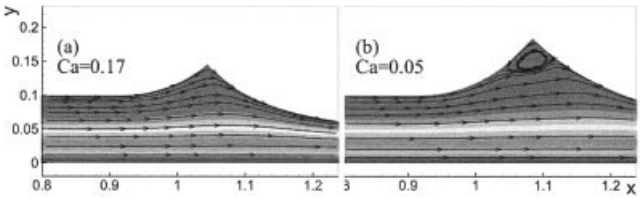

Figure 14. Comparisons of the flow field at two different capillary numbers, *Ca* = 0.17 and *Ca* = 0.05.

Uniform slot die with $R = 200$ μm. Gap-to-thickness ratio $H_0/t = 2$, and contact angle $\theta = 90^o$.

presented in all three configurations. In the divergent flow channel, the recirculation is limited to a small region under the die land close to the free surface.

Figure 17 presents the variation of the contact line position with flow rate at $R = 100$ μm, $\theta = 90^o$, and $\alpha_L = 0^o$ (parallel), $\alpha_L = -2.86^o$ (divergent), and $\alpha_L = +2.86^o$ (convergent). The coating gap configuration does not affect the contact line position while it is located along the die shoulder or the rounded edge, but has a strong effect on the position of the meniscus when the contact line is located on the die lip. The geometry with a convergent channel ($\alpha_L > 0^o$) presents clearly a turning point in the solution path at $H_0/t \approx 4.8$. Two-Dimensional solutions cannot be computed beyond this value of gap-to-thickness ratio. There is a small increase in the maximal gap-to-thickness ratio when compared to a parallel die lip configuration. This occurs because the edge angle of the die is smaller in this case, enhancing the apparent pinning effect, as described in Figure 4 and Eq. 1.

The die configuration with divergent flow channel ($\alpha_L < 0^o$) has no limit on the gap-to-thickness ratio; the sensitivity of the contact line position to the film thickness is a function of the inclination angle of the die land. As mentioned before, when the die lip is parallel to the web, there is no clear turning point, but a limit of the gap-to-thickness ratio can be determined asymptotically, as a degenerated turning point.

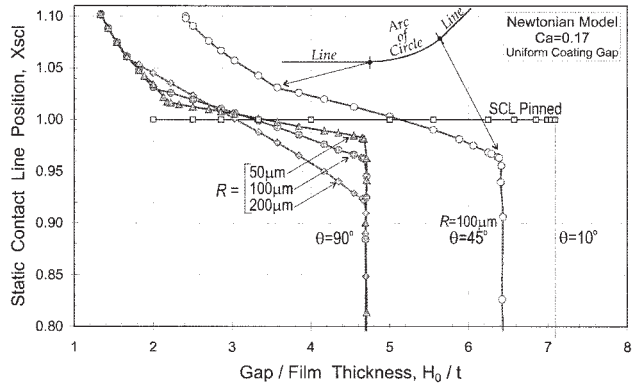

Figure 15. Static contact line position X_{scl} at different flow rates and radii of curvature ($R = 50$ μm, $R = 100$ μm, and $R = 200$ μm) of the die edge in a uniform slot coating gap with $H_0 = 100$ μm.

The free surface meets the solid wall at $\theta = 90^o$ and $\theta = 45^o$, and is free to slide along it. Newtonian liquid with $Ca = 0.17$.

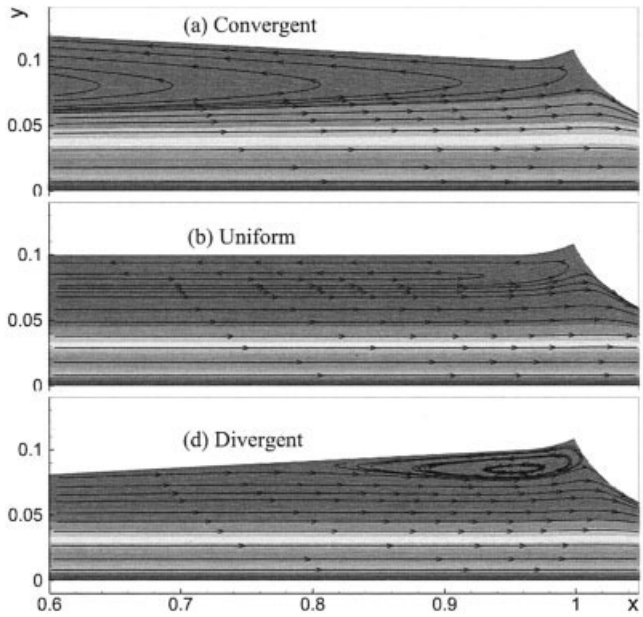

Figure 16. Influence of the angle of the die lip in the flow field. Comparisons are for $H_0/t = 3.33$, $X_{scl} = 1$, $R = 100$ μm, prescribed contact angle $\theta = 90^o$, and capillary number $Ca = 0.17$.

Conclusions

Slot coating is one of the preferred methods for high precision coating. There is an important operating limit, known as the low-flow limit, when thin films are coated at relatively high speeds. It is caused by the receding action of the downstream free surface as the flow rate is reduced at a fixed substrate speed. This operating limit and the uniformity of the coated liquid layer in the cross web direction depend on how the static contact line moves along the die surface.

It is usual practice to create edges or surface discontinuities on coating applicators in order to enhance the contact angle hysteresis and, consequently, reduce the mobility of the contact

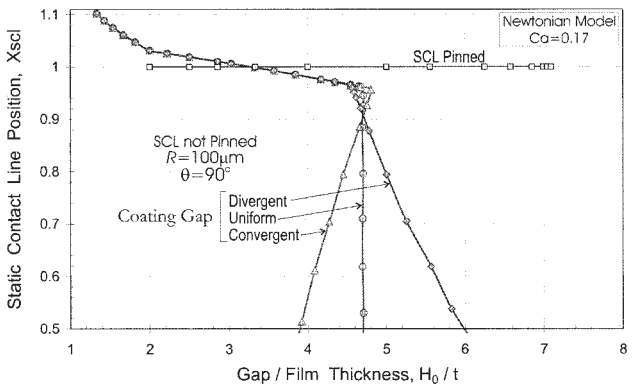

Figure 17. Static contact line position X_{scl} for coating dies with different die lip angle: $\alpha_L = -2.86^o$ (divergent), $\alpha_L = 0^o$ (uniform), and $\alpha_L = +2.86^o$ (convergent), and same radius of curvature $R = 100$ μm.

Newtonian liquid with $Ca = 0.17$.

line, causing an apparent pinning effect. Coating die edges are not mathematical corners and they have a specified radius of curvature, which is determined by machining requirements. The effect of the radius of curvature of the edge between the downstream die lip and shoulder in a slot coating applicator on the position of the contact line and on the onset of the low-flow limit is examined theoretically.

The theoretical predictions confirm that sharp die edges reduce the mobility of the contact line (apparent pinning), as is well known, and show the minimum value of the radius of curvature of die edges at which the variation of the contact line position becomes sufficiently small. The results also show that the critical condition at the low-flow limit is not affected by the die edge radius, but it is strongly affected by the static contact angle of the coating liquid.

Literature Cited

1. Beguin AL. Method of Coating Strip Material. U.S. Patent No. 2 681 294; 1954.
2. Romero OJ, Suszynski WJ, Scriven LE, Carvalho MS. Low-flow limit in slot coating of dilute solutions of high molecular weight polymer. *Journal of Non-Newtonian Fluid Mechanics.* 2004;118:137-156.
3. Ruschak KJ. Limiting flow in a pre-metered coating device. *Chemical Engineering Science.* 1976;31:1057-1060.
4. Silliman WJ. Viscous Film Flows with Contact Lines: Finite Element Simulations, A Basis for Stability Assessment and Design Optimization. Ph.D. thesis, University of Minnesota, MN, USA, 1979.
5. Higgins BJ, Scriven LE. Capillary pressure and viscous pressure drop set bounds on coating bead operability. *Chemical Engineering Science.* 1980;35:673-682.
6. Sartor L. Slot Coating: Fluid Mechanics and Die Design. Ph.D. thesis, University of Minnesota, MN, USA, 1990.
7. Gates I, Scriven LE. Stability Analysis of Slot Coating Flows. AIChE Spring National Meeting, New Orleans, 1996.
8. Carvalho MS, Kheshgi HS. Low-flow limit in slot coating: theory and Experiments. *AIChE Journal.* 2000;46:1907-1917.
9. Romero OJ, Scriven LE, Carvalho MS. Slot coating of mildly viscoelastic liquids. *Journal of Non-Newtonian Fluid Mechanics.* To appear.
10. Oliver JF, Huh C, Mason SG. Resistance to spreading of liquids by sharp edges. *Journal of Colloid and Interface Science.* 1977;59,3:568-581.
11. Maier GW, Brown OD. Die Coating Apparatus with Surface Covering. U.S. Patent No. 5 759 274; 1998.
12. Fahrni F, Zimmermann A. Coating device. U.S. Patent No. 4 109 611; 1978.
13. Gibbs JW. *Scientific Papers of J. Willard Gibbs. Volume I Thermodynamics*. New York: Dover Publications; 1961.
14. Yapel RA, Milbourn TM, Hanke RA, Goenaga A, Ebensperger ME. Coating die grinding and finishing method. U.S. Patent No. 5 655 948; 1997.
15. de Santos JM. Two-phase concurrent downflow through constricted passages. Ph.D. thesis, University of Minnesota, MN, USA, 1991.
16. Bolstad JH, Keller HB. A multigrid continuation method for elliptic problems with folds. *SIAM Journal of Scientific Stat Comput.* 1986; 7,4:1081-1104.
17. Keller HB. Numerical solution of bifurcation and nonlinear eingenvalue problems. In: Rabinowitz PH, ed. *Applications of Bifurcation Theory*. New York: Dekker; 1977.

Manuscript received May 6, 2005, and revision received July 15, 2005.